Synthesis of Mn-Doped ZnSe-ZnS Alloy Quantum Dots by a Hydrothermal Method

Hisaaki Nishimura,[1] Yuxin Lin,[1] Masayuki Hizume,[1] Taichi Taniguchi,[1] Naoteru Shigekawa,[1]
Tomomi Takagi,[2] Susumu Sobue,[2] Shoichi Kawai,[2] Eiichi Okuno,[2] and DaeGwi Kim*[1]

[1]*Department of Applied Physics, Graduate School of Engineering, Osaka City University,*
3-3-138 Sugimoto, Sumiyoshi-ku, Osaka 558-8585, Japan
[2]*Advanced Research and Innovation Center, DENSO CORPORATION,*
500-1 Minamiyama, Komenoki-cho, Nisshin, Aichi 470-0111, Japan

E-mail: tegi@a-phys.eng.osaka-cu.ac.jp

This study aims to report the hydrothermal synthesis of water-soluble Mn-doped ZnSe-ZnS alloy quantum dots (QDs), wherein manganese (Mn^{2+}) serves as an emission center. The alloy composition was controlled by the mixing ratio of ZnSe:Mn and ZnS:Mn precursor solutions. The photoluminescence (PL) band originating from the d-d transition in Mn^{2+} was clearly observed. With an increase in the amount of ZnS in the alloy QDs, the absorption onset energy shifted toward higher energy, demonstrating the successful preparation of alloy QDs, and Mn PL intensity increased as well.

Energy limitations should be overcome for the realization of a sustainable society. Power generation using solar cells is important to achieve renewable energy. Among solar cells, silicon (Si)-type solar cells are the most widespread. While Si-type solar cells effectively use light in the visible to near-infrared region for photoelectric conversion, their spectral sensitivity to ultraviolet light is low. Recently, wavelength conversion materials that convert ultraviolet light to visible light have been developed to improve the photoelectric conversion efficiency of Si-type solar cells.[1–6]

Mn^{2+}-doped ZnSe quantum dots (QDs) show potential as a wavelength conversion material because ZnSe absorbs light in the blue to ultraviolet region[7–9] and exhibits orange emission as a result of the d-d transition in the emission center of Mn^{2+}.[10-13] In our previous study, we reported the hydrothermal synthesis of water-soluble ZnSe:Mn QDs with a photoluminescence (PL) quantum yield of 20% under optimal conditions.[13] The PL quantum yield was further increased to 30% by preparing ZnSe:Mn/ZnS core/shell QDs. However, although the absorption onset energy of hydrothermally prepared ZnSe:Mn QDs shifts toward lower energy with an increase in the reaction time (i.e., as the mean QD diameter increases), the Mn PL intensity also depends strongly on reaction time. Therefore, since ZnSe:Mn QDs synthesized for a specific time (15 min) exhibit the maximum Mn PL intensity, it is difficult to control the absorption onset energy by modulating the QD diameter while maintaining a high Mn PL intensity.

This study focuses on Mn^{2+}-doped ZnSeS QDs, which are alloy semiconductors of ZnSe and ZnS. The bandgap energies of alloy semiconductors can be controlled over a wide range by changing the alloy composition.[14–18] Thus, ZnSeS:Mn QDs have the potential to exhibit high Mn PL intensity along with controlled absorption energy based on the alloy composition.

Herein, ZnSeS:Mn QDs were hydrothermally synthesized as follows. First, two precursor solutions of ZnSe:Mn and ZnS:Mn were separately prepared via a procedure similar to a previous study.[13] Briefly, $Zn(ClO_4)_2 \cdot 6H_2O$ (1.0 mmol), N-acetyl-L-cysteine (4.8 mmol) as a ligand, and $Mn(ClO_4)_2 \cdot 6H_2O$ (0.02 mmol) were dissolved in 50 mL deionized water. The pH of the aqueous solution was then adjusted to a pH of 8.5 (5.0), and a freshly prepared solution of NaHSe (Na_2S; 0.2 mmol) was added to prepare the ZnSe:Mn (ZnS:Mn) precursor solution. Subsequently, the pH of each precursor solution was adjusted to 10.0. $ZnSe_{x'}S_{1-x'}$:Mn precursor solution was prepared by mixing the ZnSe:Mn and ZnS:Mn precursor solutions, where x' denotes the mixing ratio of two precursor solutions. Finally, 10 mL of the precursor solution was loaded into a glass reactor (autoclave) and incubated at 200 °C for a specified period and then cooled to room temperature. All reaction solutions were used for various measurements without further purification.

The absorption and PL spectra of the sample solutions were recorded using a JASCO V-650 ultraviolet/visible spectrophotometer and JASCO FP-8300 spectrofluorometer, respectively. The excitation wavelength was fixed at 325 nm. The PL intensity of each sample was compared by dividing the PL intensity by the absorption intensity at the excitation wavelength. X-ray diffraction (XRD) spectra were collected using a Rigaku SmartLab diffractometer equipped with a Cu-Kα radiation source ($\lambda =$ 0.154 nm).

Figure 1 shows the absorption and PL spectra of ZnSe:Mn QDs ($x' = 1$) synthesized from the ZnSe:Mn precursor solution for reaction times of 5, 10, 15, and 20 min. In the absorption spectra, absorption structures are observed at energies above the bandgap energy of bulk ZnSe (2.7 eV), indicating the successful preparation of QDs. The PL spectra clearly show that the Mn PL intensity was maximized in the sample synthesized for 15 min. As shown in Figures S2 and S3, the Mn PL intensities of $ZnSe_{x'}S_{1-x'}$:Mn QDs, where $x' = 0.6$ and 0.8, were also maximized at the reaction time of 15 min.

Figure 2(a) shows the absorption spectra of $ZnSe_{x'}S_{1-x'}$:Mn QDs, where $x' = 0.6$, 0.8, and 1, synthesized with a reaction time of 15 min. The absorption energy was shifted toward higher energy for $x' = 0.6$ and 0.8, in comparison with that for $x' = 1$, suggesting that the alloy composition of the QDs can be controlled by varying the mixing ratio of the ZnS:Mn and ZnSe:Mn precursor solutions. XRD was used to determine the alloy compositions of the ZnSeS:Mn QDs (Figure 3). Three diffraction peaks corresponding to the (111), (220), (311) planes of the cubic zinc-blende structure were observed, and each peak is shifted toward higher angle with a decrease in x', again demonstrating the successful preparation of alloy ZnSeS QDs. For each QD
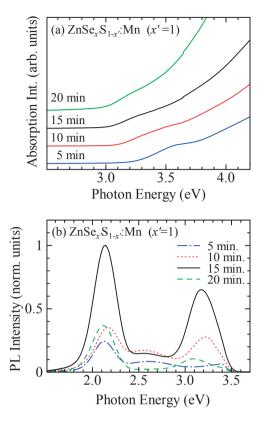
Figure 1. (a) Absorption and (b) PL spectra of ZnSe:Mn QDs synthesized with reaction times of 5, 10, 15, and 20 min.

Figure 2. (a) Absorption and (b) PL spectra of $ZnSe_{x'}S_{1-x'}$:Mn QDs, where $x' = 0.6$, 0.8, and 1, synthesized with the reaction time of 15 min.

sample, the lattice constant was calculated from the diffraction angle of the (111) plane using Bragg's law, and the actual alloy composition (x) was estimated using Vegard's law. The alloy compositions of $ZnSe_{x'}S_{1-x}$:Mn QDs for $x' = 0.8$ and 0.6 were determined to be $x = 0.80$ and 0.64, respectively. These results indicate that the alloy composition of the ZnSeS:Mn QDs can be controlled by altering the mixing ratio of the ZnSe:Mn and ZnS:Mn precursor solutions, and the absorption energy of the ZnSeS:Mn QDs can be controlled based on the alloy composition.

Figure 2(b) shows the PL spectra of the $ZnSe_{x}S_{1-x}$:Mn QDs for $x = 0.64$, 0.80, and 1. In the case where $x = 0.80$ and 0.64, the band edge PL energy is shifted toward higher energy in comparison to that in the ZnSe:Mn QDs. This phenomenon corresponds to an increase in the absorption energy with a decrease in x, as noted above when discussing Figure 2(a). On the contrary, the PL of Mn is observed at approximately 2.1 eV for all alloy compositions since it originates from the d-d transition in the emission center of Mn^{2+}.[10–12] The intensity of the Mn PL increases with a decrease in x.

Finally, $ZnSe_{0.64}S_{0.36}$:Mn/ZnS core/shell QDs were prepared by covering the surfaces of the $ZnSe_{0.64}S_{0.36}$:Mn QDs, which exhibited the highest Mn PL intensity, with ZnS shell layers. The core/shell structure is expected to suppress non-radiative recombination on the surfaces of the QDs and enhance the PL intensity.[19–21] Figure 4 shows the PL spectra of the $ZnSe_{0.64}S_{0.36}$:Mn core QDs, as shown by dashed curve, and the $ZnSe_{0.64}S_{0.36}$:Mn/ZnS core/shell QDs, as shown by solid curve. The Mn PL intensity of the $ZnSe_{0.64}S_{0.36}$:Mn/ZnS core/shell QDs was 1.4 times higher than that of the core QDs.
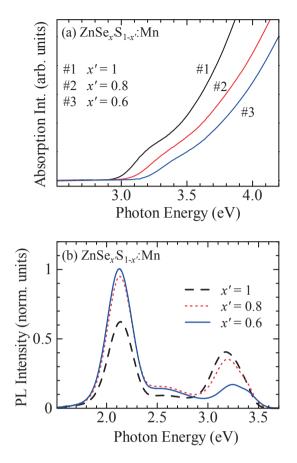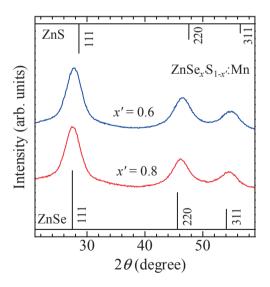

Figure 3. XRD patterns of $ZnSe_{x'}S_{1-x'}$:Mn QDs, where $x' = 0.6$ and 0.8 (JCPDS Card No. 80-0021 for ZnSe and 05-0566 for ZnS).

In summary, we hydrothermally synthesized Mn-doped alloy QDs wherein Mn^{2+} serves as the emission center to prepare QDs exhibiting high Mn PL intensity and controllable
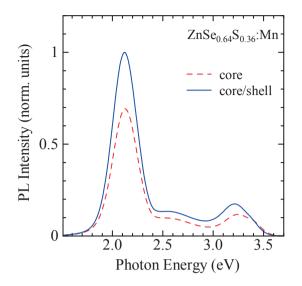
Figure 4. PL spectra of $ZnSe_{0.64}S_{0.36}$:Mn core QDs (dashed curve) and $ZnSe_{0.64}S_{0.36}$:Mn/ZnS core/shell QDs (solid curve).

absorption energy based on the alloy composition. We successfully controlled the alloy composition in the $ZnSe_xS_{1-x}$:Mn QDs and absorption energy by altering the mixing ratio of the ZnSe:Mn and ZnS:Mn precursor solutions. The Mn PL intensity increased with a decrease in x. Finally, the Mn PL intensity was increased by 1.4 times by coating the surfaces of $ZnSe_{0.64}S_{0.36}$:Mn core QDs with ZnS shells to create $ZnSe_{0.64}S_{0.36}$:Mn/ZnS core/shell QDs.

References
1   T. Trupke, M. A. Green, P. Würfel, *J. Appl. Phys.* **2002**, *92*, 1668.
2   B. S. Richards, *Sol. Energy Mater. Sol. Cells* **2006**, *90*, 1189.
3   E. Klampaftis, D. Ross, K. R. McIntosh, B. S. Richards, *Sol. Energy Mater. Sol. Cells* **2009**, *93*, 1182.
4   E. Klampaftis, B. S. Richards, *Prog. Photovoltaics* **2011**, *19*, 345.
5   X. Pi, Q. Li, D. Li, D. Yang, *Sol. Energy Mater. Sol. Cells* **2011**, *95*, 2941.
6   D.-C. Cheng, H.-C. Hao, M. Zhang, W. Shi, M. Lu, *Nanoscale Res. Lett.* **2013**, *8*, 291.
7   D. Zhao, J.-T. Li, F. Gao, C. Zhang, Z. He, *RSC Adv.* **2014**, *4*, 47005.
8   Y.-S. Lee, H.-B. Bu, T. Taniguchi, T. Takagi, S. Sobue, H. Yamada, T. Iwaki, D. G. Kim, *Chem. Lett.* **2016**, *45*, 878.
9   Y.-S. Lee, K. Nakano, H.-B. Bu, D. G. Kim, *Appl. Phys. Express* **2017**, *10*, 065001.
10 R. N. Bhargava, D. Gallagher, X. Hong, A. Nurmikko, *Phys. Rev. Lett.* **1994**, *72*, 416.
11 C. Gan, Y. Zhang, D. Battaglia, X. Peng, M. Xiao, *Appl. Phys. Lett.* **2008**, *92*, 241111.
12 R. Zeng, T. Zhang, G. Dai, B. Zou, *J. Phys. Chem. C* **2011**, *115*, 3005.
13 H. Nishimura, Y. Lin, M. Hizume, T. Taniguchi, N. Shigekawa, T. Takagi, S. Sobue, S. Kawai, E. Okuno, D. G. Kim, *AIP Adv.* **2019**, *9*, 025223.
14 K. Tomihira, D. Kim, M. Nakayama, *J. Lumin.* **2005**, *112*, 131.
15 D. G. Kim, A. Nabeshima, M. Nakayama, *Jpn. J. Appl. Phys.* **2005**, *44*, 1514.
16 M. W. DeGroot, H. Rösner, J. F. Corrigan, *Chem.—Eur. J.* **2006**, *12*, 1547.
17 J. Cheng, D. Li, T. Cheng, B. Ren, G. Qang, J. Li, *J. Alloys Compd.* **2014**, *589*, 539.
18 L. Jing, S. V. Kershaw, Y. Li, X. Huang, Y. Li, A. L. Rogach, M. Gao, *Chem. Rev.* **2016**, *116*, 10623.
19 B. O. Dabbousi, J. Rodriguez-Viejo, F. V. Mikulec, J. R. Heine, H. Mattoussi, R. Ober, K. F. Jensen, M. G. Bawendi, *J. Phys. Chem. B* **1997**, *101*, 9463.
20 V. V. Nikesh, S. Mahamuni, *Semicond. Sci. Technol.* **2001**, *16*, 687.
21 L. Li, A. Pandey, D. J. Werder, B. P. Khanal, J. M. Pietryga, V. I. Klimov, *J. Am. Chem. Soc.* **2011**, *133*, 1176.